

# Mechanisms of adherence of alumina scale developed during high-temperature oxidation of Fe-Ni-Cr-Al-Y alloys

D. DELAUNAY, A. M. HUNTZ

*Laboratoire de Métallurgie Physique, LA No. 177, Université de Paris-Sud, 91405 Orsay, France*

By studying the beneficial effect of yttrium for high-temperature cyclic oxidation resistance of Fe-Ni-Cr-Al alloys, the mechanisms responsible for alumina scale-substrate adherence are approached, discussed and pointed out in this particular case. The principal mechanisms proposed by various authors are examined, taking into account results and observations obtained by oxidizing these alloys. Some of the assumptions usually put forward, particularly that of mechanical keying of the oxide scale by yttria particles, are excluded in this case, while others, such as the influence of yttrium on the oxide stresses, seem to be preponderant. Indeed, various experiments show that yttrium additions improve oxide scale adherence by increasing alumina plasticity. This effect is related to the influence of yttrium on the cationic mobility in alumina.

## 1. Introduction

The isothermal oxidation behaviour of high-temperature-resistant alloys has been extensively studied. It is clear that alloys which develop an alumina scale are more resistant than alloys which develop a chromia scale. Besides, addition elements at low contents, such as rare-earth elements, Hf, Y, etc., improve the oxidation resistance of the alloy by decreasing the oxidation rate, and especially, by improving the oxide scale adherence. Indeed, oxide spalling has a disastrous effect on the protective nature of the oxide, and consequently on the life span of the alloy. While the beneficial influence of additional elements, such as yttrium, is easily recognized, the adherence mechanisms on the other hand are rarely explained. The main mechanisms put forward are as follows:

(a) Yttrium (or other addition elements) can improve the chemical bonds at the oxide-metal interface. Indeed, its oxygen affinity is greater than the oxygen affinity of other alloy elements.

(b) Yttride precipitates or yttria particles can induce mechanical keying of the oxide scale on the substrate.

(c) Yttrium can promote the formation of

either an inner yttria layer or an inner oxide layer, mainly made of yttria with alumina or chromia. This intermediate layer can act as a diffusion barrier or decrease the mechanical or thermal stresses between the oxide scale and the alloy.

(d) Soluble yttrium in the alloy can trap the metal vacancies and, consequently avoid vacancy coalescence at the metal-oxide interface, which promotes oxide spallings.

(e) Yttrium present in the oxide scale can influence oxide defect mobility and, consequently, diffusion rate in the oxide scale, oxide thickness and plasticity.

On the basis of results that we obtained by studying the influence of yttrium, in Fe-Ni-Cr-Al alloys on high-temperature oxidation [1-7], the mechanisms leading to the beneficial influence shown by yttrium addition on oxide-metal adherence have been identified.

## 2. Oxidation study of Fe-Ni-Cr-Al alloys

The tested Fe-Ni-Cr-Al alloys contain 5 wt% aluminium, a content which allows the growth of a continuous alumina scale, 20 to 25 wt% chromium

and 20 to 45 wt% nickel; depending on the Ni-content the alloy structure is either austenitic or austenoferritic [5–7]. Yttrium additions are included between 100 and 10 000 ppm. We have previously shown [1–3] that there is an optimum yttrium content in order to obtain the best resistance to oxidation and a good oxide adherence. This content is about 100 to 300 ppm, depending on the alloy composition (Fig. 1), and seems to be fairly similar to the yttrium solubility limit in these alloys.

The oxide scale is made up of two layers (see Fig. 2): an outer layer of  $\text{Cr}_2\text{O}_3$  and spinel oxide,  $\text{NiO}$  ( $\text{Fe, Al, Cr}$ ) $_2\text{O}_3$  (this layer is enriched in Mn) and an inner layer of columnar grains of alumina enriched in yttria. The relative importance of these layers depends on the alloy structure and oxidation treatment (Fig. 2). Yttrium was never

detected in the outer scale [3]. Alumina mainly grows by anionic diffusion [8].

Experiments were carried out in yttrium-implanted specimens [9] and showed that the oxidation behaviour of implanted alloys is fairly similar to the as-cast alloy behaviour. Furthermore, after the oxidation treatment, all the implanted yttrium is localized within the  $\text{Al}_2\text{O}_3$  layer. Pegging by yttria particles was never observed. Therefore, it can be assumed that the yttrium influence on oxide adherence is related to the presence of soluble yttria in alumina scale.

### 3. Examination of the various adherence mechanisms

On the basis of various studies related to the oxidation behaviour of Fe–Ni–Cr–Al alloys [1–7, 9], the validity of the various possible mech-

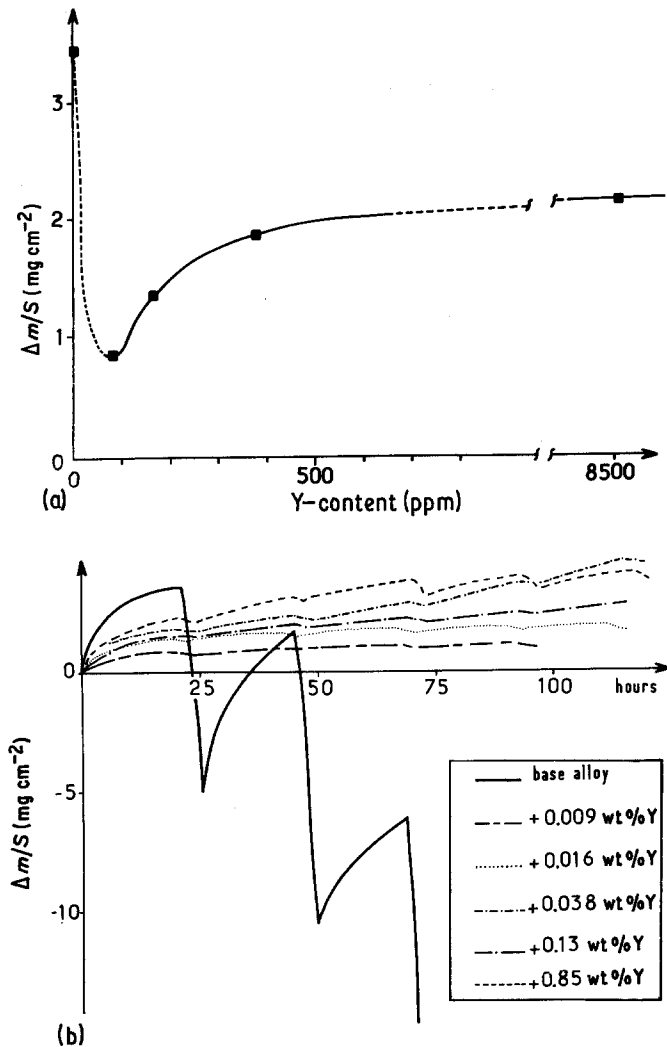


Figure 1 (a) Weight-gain variation per unit surface,  $\Delta m/s$ , of  $\text{FeNi}_{4.5}\text{Cr}_{2.5}\text{Al}_5$  alloys oxidized for 20 h at  $1300^\circ\text{C}$ , plotted against yttrium content. The optimum content seems to be near 90 ppm. (b) The influence of yttrium additions on cyclic oxidation of  $\text{FeNi}_{4.5}\text{Cr}_{2.5}\text{Al}_5$  alloys. Cycles made up of an isothermal oxidation for 20 h at  $1300^\circ\text{C}$  and a cooling down to  $260^\circ\text{C}$  (4 h).

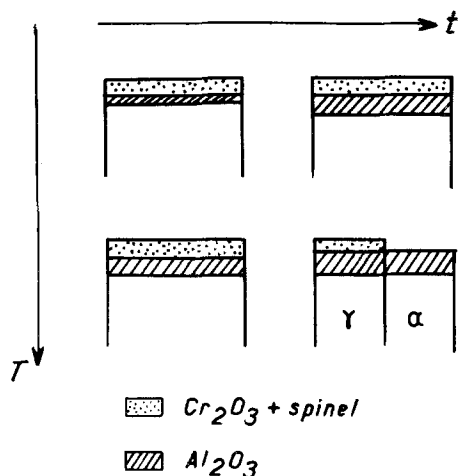


Figure 2 Schematic diagram of the composition of the oxide scales developed on Fe–Ni–Cr–Al alloys in relation to their structure and to oxidation time,  $t$ , and temperature,  $T$ .

ansims mentioned above can be considered, in order to interpret the beneficial influence of yttrium.

### 3.1. Improvement of chemical bonding at the oxide–metal interface

This assumption is rarely proposed and does not seem adequate on account of the low soluble yttrium content at the oxide–metal interface. On this hypothesis, increase of yttrium content would induce an improvement of the adherence; this was not found to be the case in our alloys.

### 3.2. Mechanical keying of the oxide scale

In the case of the Fe–Ni–Cr–Al alloys tested [1–7], this mechanism is excluded. Pegging by yttria particles was never observed. On the contrary, spalling preferentially occurs along alloy grain boundaries where yttrides precipitate (see Fig. 3).

### 3.3. Intermediate layer formation

The development of an intermediate layer, enriched in yttrium, which reduces the substantial mechanical property variations at the oxide–substrate interface, is often used for silicon-based devices in the semiconductor industry. In the case of yttrium-doped alloys, which develop an inner  $\text{Al}_2\text{O}_3$  layer, such an intermediate layer has not been observed up to now. It is clear that, taking into account the low yttrium content, such a layer would be very thin and difficult to detect.

Moreover, it must be mentioned that the chemical and mechanical properties of yttria are not suitable for this kind of utilization on Fe–Ni–Cr–Al alloys.

### 3.4. Vacancy trapping

This assumption is frequently proposed [10–13] but relies only on micrographic observations. Indeed, the influence of yttrium is often related to a porosity decrease at the oxide–metal interface. Such porosity is characteristic and has often been observed on Fe–Ni–Cr–Al alloys, without yttrium, after a long oxidation treatment at high temperature. Fig. 4, relative to the oxide–metal interface observation, shows one of these pores which appear as a smooth area (surrounded by alumina imprints). These smooth areas attest an adherence loss during oxidation, as shown by the thermal etching, and are large (diameter,  $\phi \approx 20$  to  $30 \mu\text{m}$ , while the alumina grain diameter is about 2 to  $5 \mu\text{m}$ ). Thus, it seems difficult to attribute them to the vacancy coalescence phenomenon alone. Nevertheless, these spallings may have initiated along coalescence sites. A large number of observations allow us to be sure that the number of smooth areas is much lower in yttrium-doped alloys than in undoped alloys.

### 3.5. Influence on defect mobility

If yttrium traps the metal vacancies and prevents their coalescence at the oxide–metal interface, then this element increases the oxide adherence by acting on oxide defect mobility and on plasticity. In such a case it must be expected that yttrium decreases the stresses in the oxide scale. In order to verify this assumption the mechanical behaviour of alumina scales was studied.

## 4. Mechanical behaviour of alumina scales

By now, many authors have sought to emphasize the mechanical aspects of oxidation; relations have to be established between the protective nature of oxides and their behaviour when submitted to mechanical forces during oxidation. Inversely, the mechanical properties of the metal–oxide system must be related to the oxidation kinetics of the alloys.

Parameters which can induce stresses in the oxide or subjacent metal are particularly numerous and have been described in recent review papers [4, 14]: the Pilling and Bedworth ratio [15], epitaxial phenomena, alloy and oxide composition

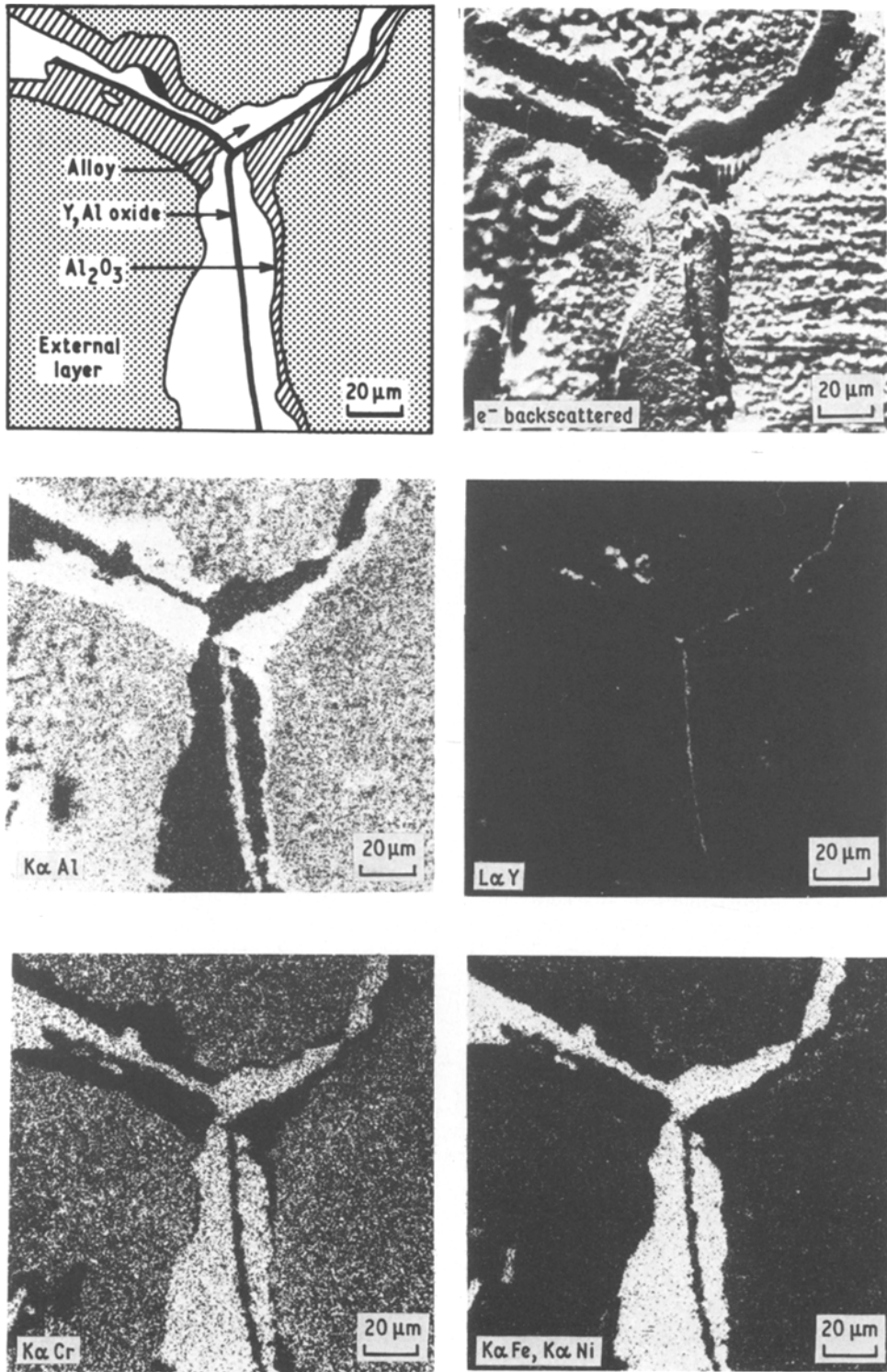


*Figure 3* Observation of oxide spalling along alloy grain boundaries enriched in yttrium. FeNi<sub>4.5</sub>Cr<sub>2.5</sub>Al<sub>5</sub>Y<sub>0.1</sub> oxidized for 50 h at 1200° C.

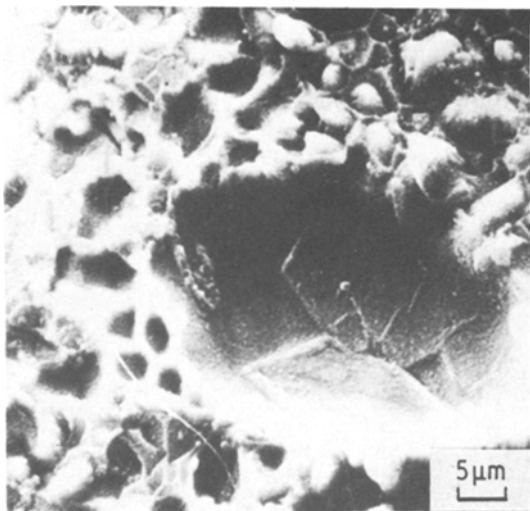


Figure 4 Scanning electron micrograph of metal-oxide interface of FeNi<sub>4.5</sub>Cr<sub>2.5</sub>Al<sub>5</sub> alloy oxidized at 1300°C. For undoped alloys, such smooth areas revealing an adherence loss during isothermal oxidation are frequently observed.

or structure, nature of defects, thermal expansion coefficients all have an influence on the induced stresses during oxidation. In addition, stress relaxation can occur during oxidation, induced by several mechanisms that can be separated into three classes:

(a) oxide film breakdown which can appear by disastrous oxide cracks or spallings;

(b) plastic deformation of the metallic matrix; and

(c) plastic deformation of the oxide; indeed, in spite of the brittle character of Cr<sub>2</sub>O<sub>3</sub> or Al<sub>2</sub>O<sub>3</sub> at low temperatures, induced stresses can be sufficient to induce a plastic deformation at high oxidation temperatures.

Experimental tests developed, up to now, in order to measure oxide stresses or stresses relaxation are not satisfactory. Two types of techniques can be considered:

(1) tests on massive oxide specimens; and

(2) *in situ* techniques, intended to characterize the mechanical behaviour of the oxide as oxidation is going forward.

These two types of techniques give complementary information, but it is clear that, up to now, measured values during oxidation are not really significant; they are related to many parameters and, particularly, to the sample geometry imposed by the experimental procedure. Conversely, measured values on synthetic oxides are

significant but not representative of the same oxides grown on a metallic base.

Amongst all the procedures used [16–33], we have selected the principle of deflection measurements during unilateral oxidation. This test (*in situ* procedure) involves measuring the deflection of a thin metallic foil protected on one side and oxidized on the other [20]. Its efficiency relies on the protective nature of the coating. In our case, we found that a sputtering of a thin ( $\approx 600$  nm) crystallized silica film gives an effective protection for our alloys for oxidation times of up to 1 h at 1100°C; silica is more protective than other coatings used by various investigators.

Fig. 5 shows a schematic diagram of the apparatus developed for deflection measurements on samples of dimensions 40 mm × 11 mm × 0.15 mm samples, and already described elsewhere [4]. The deflection value,  $D$ , can be related to the oxide stress  $\sigma_{\text{ox}}$  according to the empirical Norin formula [18, 34]:

$$\sigma_{\text{ox}} = \frac{E}{1-\nu^2} \frac{1}{3L^2} \frac{e^2 D}{X_{\text{ox}}},$$

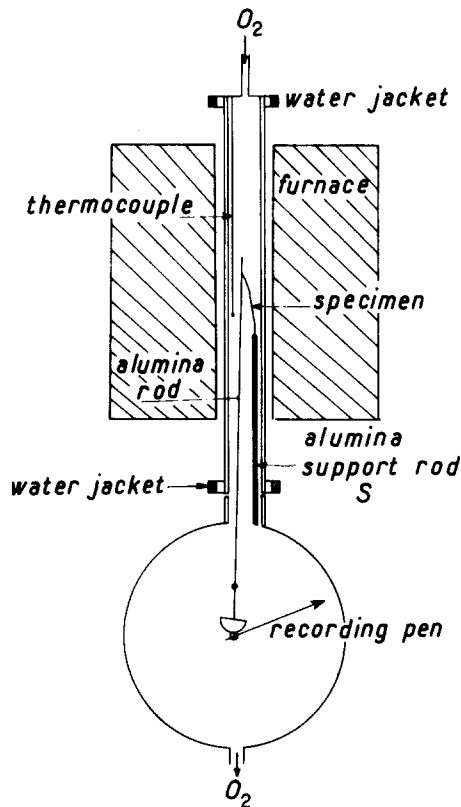


Figure 5 Schematic diagram of the deflection measurement apparatus which allows the oxide stresses,  $\sigma$ , to be deduced.

where  $X_{ox}$  is the oxide thickness,  $E$  is Young's modulus of the alloy,  $\nu$  is Poisson's ratio of the alloy,  $L$  is the initial length of the sample and  $e$  is the thickness of the sample. Thus, this technique allows measurement of the oxide  $\sigma$ -value for undoped or yttrium-doped Fe–Ni–Cr–Al alloys, and to establish whether the beneficial effects of yttrium additions on oxide adherence are related to a decrease of the oxide stresses when yttrium is present in the oxide scale. Fig. 6 shows experimental deflection curves obtained at 1000°C and the variation of  $\sigma_{ox}$  against  $X_{ox}$  is given in Fig. 7. The form of these curves agrees with previous works [18, 34] and shows that compressive stresses appear in the oxide; the high  $\sigma$ -values obtained at the beginning of the oxidation can be associated with epitaxial relationships between the oxide scale and the matrix [18]. It is clear that a 90 ppm yttrium addition in the alloy induces a notable decrease of oxide  $\sigma$ -value. During cooling, deflection increases substantially (Fig. 6); the curvature is a linear function of the temperature decrease and, by re-treating, the sample progressively returns to the same curvature as before cooling. This reversible deformation is mainly due to differences of the thermal expansion coefficients between the oxide and metallic matrix; yttrium addition does not influence these anisothermal stresses. The relative importance of anisothermal stresses is comparable with that of growth (isothermal) stresses. Nevertheless, oxide spalling preferentially occurs during cooling at about 800 to 700°C. On account of these two observations, it can be assumed that the protective nature of the oxide at high temperature

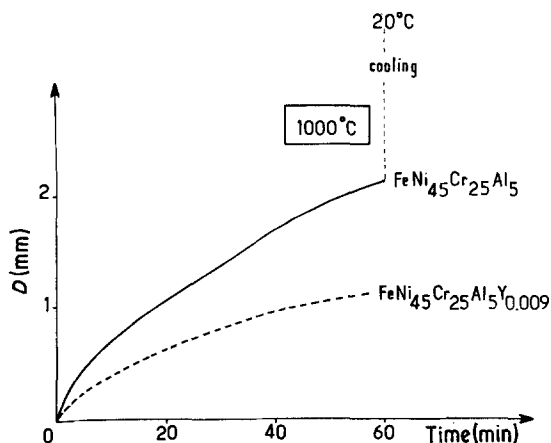


Figure 6 Deflection variation plotted against oxidation time. Influence of yttrium on isothermal deflection of FeNi<sub>45</sub>Cr<sub>25</sub>Al<sub>5</sub> alloys oxidized at 1000°C.

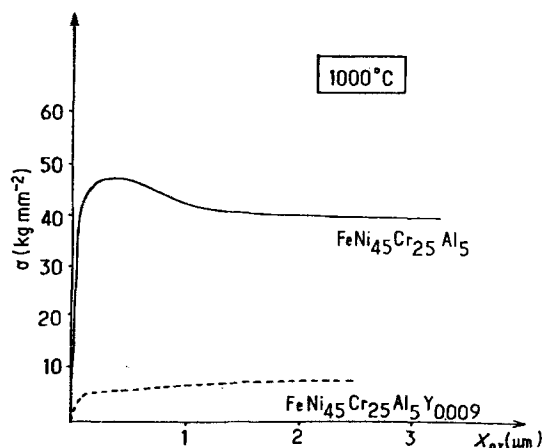


Figure 7 Oxide stress values,  $\sigma$ , plotted against oxide thickness,  $X_{ox}$ . 90 ppm yttrium addition notably decreases the oxide stress level.

is preserved by stress relaxation (due to oxide plasticity), while, during cooling, oxide plasticity decreases with temperature, oxide spalling occurs and the protective nature of the oxide is damaged. Thus, the beneficial influence of yttrium on adherence (shown by the decrease of  $\sigma$ ) must be related to an increase of oxide plasticity by yttrium. In Section 2 it was noted that the influence of yttrium on the oxide adherence is related to the presence of soluble yttria in the alumina scale. If soluble yttria improves alumina plasticity, it must also influence diffusional phenomena in alumina. In addition, the oxide–metal interface and oxide scale observations show that the optimum yttrium addition notably decreases the incidence of porosity and cracks. This aspect can also be related to the influence of yttrium on diffusional phenomena in alumina.

Before studying yttrium influence on cation mobility (see Section 5) it can be noted that the stress relaxation by plastic deformation of Al<sub>2</sub>O<sub>3</sub> can be induced by various phenomena:

- (a) dislocation climb;
- (b) Herring–Nabarro diffusion creep which would be promoted by the small Al<sub>2</sub>O<sub>3</sub> grain size (see Fig. 4); and
- (c) grain-boundary slipping which would be promoted by a columnar structure of Al<sub>2</sub>O<sub>3</sub>, [35] (see Fig. 8).

The highest stresses must be preferentially localized along grain boundaries and especially triple-points, defects in these areas acting as probable initiation sites of cracks. Yttride precipitates in grain boundaries must increase stresses;

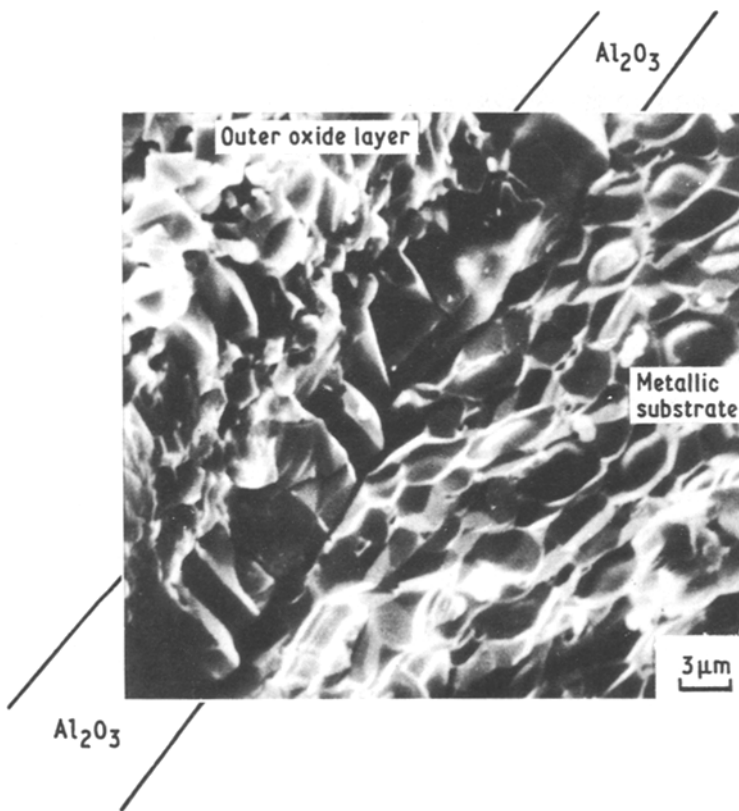


Figure 8 Observation of the oxide scale developed on  $\text{FeNi}_{4.5}\text{Cr}_{2.5}\text{Al}_5\text{Y}_{0.016}$  oxidized for 100 h at  $1300^\circ\text{C}$ . The inner alumina layer has a columnar structure.

that would explain the adherence loss preferentially observed along grain boundaries when the yttrium is increased in the alloy.

### 5. Yttrium influence on diffusional phenomena in alumina

The influence of yttrium on cationic mobility in alumina was studied using a radioactive tracer technique. The  $\text{Al}^{3+}$  diffusion coefficient cannot be measured by such a way [36], but it is possible to compare diffusion rate of other cations (chromium, nickel, etc.) in pure or yttrium-doped alumina. It is also possible to discover the aluminum mobility by studying the first stages of sintering of pure or yttrium-doped alumina. Indeed, it appears that the first sintering process of alumina is controlled by  $\text{Al}^{3+}$  ion diffusion [37, 38].

Sintering rate measurements of compressed samples of pure or yttrium-doped alumina were carried out by dilatometric tests [39]. Initial samples were obtained by mixing  $\text{Al}_2\text{O}_3$  and  $\text{Y}_2\text{O}_3$  powders (whose characteristics are collected in Table I), taking into account the relative

proportion of each element in the oxide scale grown on alloys tested here. Contraction curves (see Figs 9 and 10) show that yttria addition increases the sintering kinetics of alumina for yttrium additions up to 1 at % when the grain size of the initial powders is fairly equal. Thus, it appears that  $\text{Y}_2\text{O}_3$  additions in alumina promote  $\text{Al}^{3+}$  ion diffusion.

In order to confirm this yttrium effect on cationic diffusion in polycrystalline alumina, diffusion coefficient measurements of  $^{51}\text{Cr}$  in pure or yttrium-doped alumina were carried out [40, 41]\*. Alumina samples were obtained by sintering at high temperature under load and had approximately the same grain size as alumina

TABLE I Powder characteristics\*

Powder	Mean grain size (nm)	Purity (%)
$\text{Al}_2\text{O}_3$	5.0	99.995†
$\text{Y}_2\text{O}_3$	100.0	99.5

\* Purified by DJEVA.

† Provided by A. M. LEJUS (ENSC Paris) and MM. Revcolevschi and Berton (University of Paris-Sud, Orsay).

\*This part of the study was carried out in collaboration with B. Lesage and M. H. Lagrange.

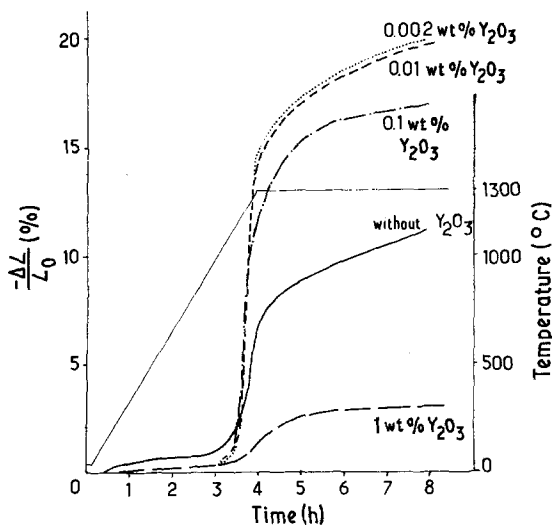


Figure 9 Influence of various yttria additions in alumina on the alumina sintering rate of 1300°C ( $\text{Al}_2\text{O}_3$ , particle size  $\approx 5.0$  nm;  $\text{Y}_2\text{O}_3$ , particle size  $\approx 100.0$  nm; and compressive pressure of 160 kg  $\text{cm}^{-2}$ ).

developed on our alloys by oxidation. Results, collected in Figs 11 and 12, show that yttria addition promotes grain-boundary diffusion; the lower the temperature, the greater this effect, perhaps related to an yttria segregation in grain boundaries. The grain-boundary diffusion increase is probably responsible for the volume-diffusion increase (Fig. 11); it must be noted that in such samples (diameter of alumina grains  $\approx 1$  to 5  $\mu\text{m}$ ), only an "apparent" volume-diffusion coefficient is

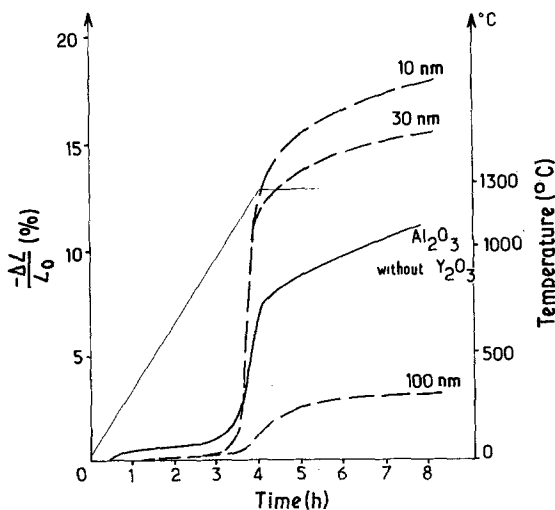


Figure 10 Influence of the yttria particles grain-size on the sintering rate at 1300°C of a  $\text{Al}_2\text{O}_3$ -1 at %  $\text{Y}_2\text{O}_3$  powders mixture. ( $\text{Al}_2\text{O}_3$ , particle size  $\approx 5.0$  nm; and compressive pressure of 160 kg  $\text{cm}^{-2}$ ).

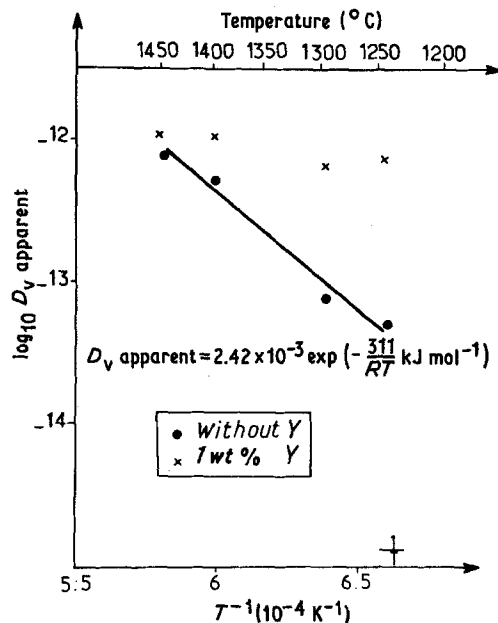


Figure 11 Variation of the "apparent" volume-diffusion coefficient of  $^{51}\text{Cr}$  in polycrystalline alumina plotted against temperature (semi-logarithmic co-ordinates) [40, 41]. Yttria presence in alumina increases the "apparent" volume-diffusion coefficient.

derived. Thus, the presence of yttrium in alumina promotes cationic mobility. This observation agrees with results obtained on the influence of yttrium on stress relaxation. Since yttrium has the

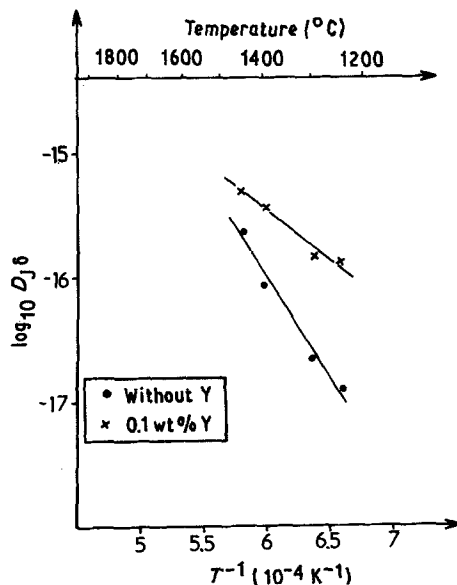


Figure 12 Variation of the grain-boundary diffusion coefficient of  $^{51}\text{Cr}$  in polycrystalline alumina plotted against temperature (semi-logarithmic co-ordinates) [40, 41]. The lower the temperature, the larger the increase of  $D_{\text{gb}}$  due to the presence of yttria in alumina.



same valence as aluminium, these two related effects must be due to its size ( $Y^{3+}$  ion diameter = 0.093 nm) which differs from the  $Al^{3+}$  size ( $Al^{3+}$  ion diameter = 0.050 nm). Being bigger, the repulsive effect of yttrium on cations must be smaller than the repulsive effect of aluminium. Such an assumption would be supported by an opposite effect on anionic mobility.

## 6. Conclusions

Mechanisms of adherence loss of oxide scales are complex and difficult to establish experimentally.

The beneficial influence of additions of active elements, such as yttrium, allows the modification of the oxidation phenomena and also permits access to information as regards oxide adherence. Nevertheless, the oxide adherence can be modified by other parameters, such as sample geometry or atmosphere. In the present work, adherence mechanisms were preferentially investigated by studying the influence of yttrium additions on the oxidation of Fe-Ni-Cr-Al alloys under fixed instrumental conditions.

In the case of these alumina-forming alloys, it is clear that yttrium does not promote mechanical keying of the oxide scale. On the contrary, if the yttrium content is great (higher than its solubility limit), yttrides precipitate along grain boundaries and act as preferential sites for spalling. Thus, mechanical keying does not appear as a mechanism responsible for the oxide adherence. When the yttrium content is limited, improvement of chemical bonding or formation of an intermediate inner oxide layer seem to be excluded.

It appears that alloy vacancy trapping by yttrium is a probable adherence mechanism since isothermal spalling, probably related to vacancy coalescence, is less frequent in yttrium-doped alloys than it is in undoped alloys. However, the mechanism mainly responsible for the oxide adherence is related to the influence of yttrium on oxide defect mobility; simultaneously, yttrium increases cationic mobility in alumina and promotes oxide stress relaxation. Alumina plasticity improvement is due to soluble yttrium.

This study shows the great importance of the mechanical characteristics on high-temperature oxidation. It is sure that oxide or substrate stresses influence oxidation kinetics and especially oxide scale adherence, that is, influence the formation of a protective oxide scale.

## References

1. J. H. DAVIDSON, P. LACOMBE, A. M. HUNTZ, C. ROQUES-CARMES, J. C. PIVIN and D. DELAUNAY, Proceedings of the International Conference on the Behaviour of High Temperature Alloys in Agressive Environments, Petten, October 1979 (Petten Establishment, 1980) p. 209.
2. J. H. DAVIDSON, "Journées d'Etudes du Comité Français d'Electrothermie", Versailles (Août, 1978).
3. J. C. PIVIN, D. DELAUNAY, C. ROQUES-CARMES, A. M. HUNTZ and P. LACOMBE, *Corrosion Sci.* **20** (1980) 351.
4. D. DELAUNAY, A. M. HUNTZ and P. LACOMBE, *Corrosion Sci.* **20** (1980) 1109.
5. D. DELAUNAY, Dr -Ing. Thesis, Paris-Sud University, Orsay, France, 1980.
6. D. DELAUNAY, A. M. HUNTZ and P. LACOMBE, *Corrosion Sci.*, to be published.
7. D. DELAUNAY and A. M. HUNTZ, to be published.
8. U. BERNABAI, M. CAVALLINI, G. BONBARA, G. DEARNELEY and M. A. WILKINS, *Corrosion Sci.* **20** (1980) 19.
9. J. C. PIVIN, C. ROQUES-CARMES, J. CHAUMONT and H. BERNAS, *ibid.* **20** (1980) 947.
10. J. D. KUENZLY and D. L. DOUGLASS, *Oxidation Met.* **8** (1974) 139.
11. J. K. TIEN and F. S. PETTIT, *Met. Trans.* **3** (1972) 1587.
12. C. S. GIGGINS and F. S. PETTIT, Pratt and Whitney Aircraft Corporation, Internal Report number ARL TR 75-0239 (1975).
13. C. S. GIGGINS, B. H. KEAR, F. S. PETTIT and J. K. TIEN, *Met. Trans.* **5** (1974) 1685.
14. D. P. WHITTLE and J. STRINGER, *Phil. Trans. Roy. Soc.* **A295** (1980) 309.
15. N. B. PILLING and R. E. BEDWORTH, *J. Inst. Met.* **29** (1923) 529.
16. B. PIERAGGI and F. DABOSI, *J. Microsc. Spectr. Elect.* **4** (1979) 595.
17. L. J. WEIRICK, in Proceedings of the Conference on Stress Effects and the Oxidation of Metals, 1974 edited by J. V. Cathcart (AIME, Philadelphia, 1974) p. 299.
18. A. NORIN, *Oxidation Met.* **9** (1975) 259.
19. W. K. APPLEBY and R. F. TYLECOTE, *Corrosion Sci.* **10** (1970) 325.
20. G. C. STONEY, *Proc. Roy. Soc.* **A82** (1909) 172.
21. D. D. DANKOV and P. V. CHURAEV, *Dokl. Akad. Nauk. SSSR* **73** (1950) 1221.
22. R. E. PAWEL, J. V. CATHCART and J. J. CAMPBELL, *J. Electrochem. Soc.* **110** (1963) 55.
23. W. JAENICKE, S. LEISTIKOW, A. STADLER and L. ALBERT, *Mem. Sci. Rev. Mét.* **LXII** (1965) 231.
24. W. JAENICKE, S. LEISTIKOW and A. STADLER, *J. Electrochem. Soc.* **111** (1964) 103.
25. P. HANCOCK, Proceedings of the Conference on Stress effects and the Oxidation of Metals, 1974, edited by J. V. Cathcart (AIME, Philadelphia, 1974) p. 155.
26. J. B. JOHNSON, J. R. NICHOLLS, R. C. HURST and P. HANCOCK, *Corrosion Sci.* **18** (1978) 527.

27. C. CODDET, J. F. CHRETIEN, G. BERANGER, *Compt. Rend. Acad. Sci. Paris C282* (1976) 815.
28. B. PIERAGGI, private communication, 1980.
29. D. L. DOUGLASS, *Corrosion Sci.* 5 (1965) 255.
30. J. L. CADOZ, PhD Thesis, Paris-Sud University, Orsay, France (1978).
31. J. L. CADOZ and B. PELLISSIER, *Scripta Met.* 10 (1976) 597.
32. H. GERVAIS, B. PELLISSIER and J. CASTAING, *Rev. Int. Hautes Temp.* 15 (1978) 43.
33. F. A. GOLIGHTLY, F. S. STOTT and G. C. WOOD, *Werkstoffe und Korrosion* 30 (1979) 487.
34. A. NORIN, Swedish Atomic Energy, Internal Report, RMM 1733 (1969), presented at the High Temperatures Symposium, Oslo, May 1969.
35. G. BERANGER and C. CODDET, *J. Microsc. Spectr. Elect.* 5 (1980) 793.
36. Y. OISHI and W. D. KINGERY, *J. Chem. Phys.* 33 (1960) 480.
37. R. L. COBLE, *J. Appl. Phys.* 32 (1961) 787.
38. G. C. KUCZYNSKI, *Trans. AIME* 185 (1949) 169.
39. D. DELAUNAY, A. M. HUNTZ and P. LACOMBE, *J. Less-Common Metals* 70 (1980) 115.
40. B. LESAGE and A. M. HUNTZ, *Scripta Met.* 14 (1980) 1143.
41. B. LESAGE, M. H. LAGRANGE, D. DELAUNAY and A. M. HUNTZ, private communication, 1980.

*Received 20 November  
and accepted 8 December 1981*